

# One at a time, live tracking of NGF axonal transport using quantum dots

Bianxiao Cui<sup>a</sup>, Chengbiao Wu<sup>b,c</sup>, Liang Chen<sup>d</sup>, Alfredo Ramirez<sup>b,c</sup>, Elaine L. Bearer<sup>e,f</sup>, Wei-Ping Li<sup>g</sup>, William C. Mobley<sup>b,c,h</sup>, and Steven Chu<sup>a,d,h,i,j,k</sup>

Departments of <sup>a</sup>Physics and <sup>b</sup>Neurology and Neurological Sciences, <sup>c</sup>Neuroscience Institute, and <sup>d</sup>Department of Applied Physics, Stanford University, Stanford, CA 94305; <sup>e</sup>Department of Pathology and Laboratory Medicine, Brown University, Providence, RI 02910; <sup>f</sup>Department of Biology, California Institute of Technology, Pasadena, CA 91125; <sup>g</sup>Department of Cell Biology, University of Texas Southwestern Medical Center, Dallas, TX 75390; <sup>i</sup>Lawrence Berkeley National Laboratory, Berkeley, CA 94720; and Departments of <sup>j</sup>Physics and <sup>k</sup>Molecular and Cell Biology, University of California, Berkeley, CA 94720

Contributed by Steven Chu, July 6, 2007 (sent for review March 19, 2007)

**Retrograde axonal transport of nerve growth factor (NGF) signals is critical for the survival, differentiation, and maintenance of peripheral sympathetic and sensory neurons and basal forebrain cholinergic neurons. However, the mechanisms by which the NGF signal is propagated from the axon terminal to the cell body are yet to be fully elucidated. To gain insight into the mechanisms, we used quantum dot-labeled NGF (QD-NGF) to track the movement of NGF in real time in compartmentalized culture of rat dorsal root ganglion (DRG) neurons. Our studies showed that active transport of NGF within the axons was characterized by rapid, unidirectional movements interrupted by frequent pauses. Almost all movements were retrograde, but short-distance anterograde movements were occasionally observed. Surprisingly, quantitative analysis at the single molecule level demonstrated that the majority of NGF-containing endosomes contained only a single NGF dimer. Electron microscopic analysis of axonal vesicles carrying QD-NGF confirmed this finding. The majority of QD-NGF was found to localize in vesicles 50–150 nm in diameter with a single lumen and no visible intraluminal membranous components. Our findings point to the possibility that a single NGF dimer is sufficient to sustain signaling during retrograde axonal transport to the cell body.**

live imaging | nerve growth factor | single molecule imaging | NGF signaling | retrograde transport

**N**erve growth factor (NGF) is produced and released by target tissues to activate specific receptors at the axon terminals of innervating neurons. In order for NGF to regulate gene expression and the survival of target neurons, a signal must be moved a considerable distance, in some cases >1,000-fold the diameter of the neuron cell body. The elucidation of the mechanism(s) used to transmit NGF signal from the terminals of axons to cell bodies of neurons is yet to be fully defined. In that retrograde NGF signaling is critical for the survival and maintenance of neurons of both the peripheral and central nervous systems, and the underlying mechanisms are likely to be shared by related neurotrophic factors, the issue remains one of the most significant and intriguing questions in neurobiology (1–16).

In the past, radio-labeled NGF (<sup>125</sup>I-NGF) has been used to study the binding, internalization, and axonal transport of NGF. These studies facilitated the measurement of transport rate and provided insights into the endocytic pathways used for NGF transport (8, 16–19). Fluorescent labels such as rhodamine (20), Texas red (21), and Cy3 (22) were also used to track NGF movement in neurons. However, because these previous methods have limited spatial and temporal resolution, they provide only a coarse look at what is expected to be a very dynamic process. Moreover, few studies have examined NGF-containing endosomes during axonal transit. Some have suggested that NGF is transported principally within early endosomes (4, 5, 7–14) whereas others suggest that NGF is transported in organelles with complex membrane structures such as multivesicular bodies (MVBs) (8, 20) and in macropinosomes (23).

Thus, how NGF is transported and in which organelle(s) are unresolved questions.

In this study, we used quantum dots (QDs) to track retrograde transport of NGF in compartmentalized cultures of rat dorsal root ganglion (DRG) neurons. Using pseudoTIRF microscopy, we tracked the movement of QD-NGF in live DRG neurons in real time. Our approach uncovered previously unappreciated details of the movement of NGF during retrograde transport. Endosomes containing QD-NGF exhibited “stop-and-go,” unidirectional retrograde motion with an average speed of  $1.31 \pm 0.03 \text{ } \mu\text{m/s}$ . Whereas our speed measurements are consistent with previous bulk studies of NGF transport (14), the ability to visualize individual endosomes revealed a great diversity of transport phenomena. Furthermore, we were able to define the number of NGF molecules contained in individual endosomes. Together with electron microscopy analysis, we found that the vast majority of endosomes contained a single NGF dimer at physiological concentrations, and that small vesicles (50–150 nm in diameter) contained >95% of NGF.

## Results

**QD-NGF Is Fully Biologically Active.** QDs are revolutionary fluorescent probes with excellent photostability (24). When combined with ultrasensitive optical techniques, QDs allow tracking of individual biomolecules in live cells with high signal-to-noise ratio and over unprecedented durations (25–27). We examined retrograde transport of NGF-containing vesicles by using QD-NGF to mark these organelles. Purified NGF (28) was biotinylated (BtNGF) according to published protocols (29, 30). On average, each dimer of BtNGF contains 3 biotin additions. BtNGF was conjugated to QD-streptavidin by mixing on ice overnight with a molar ratio of BtNGF dimer to QD of 1 to 1.2. As assayed by SDS/PAGE gel, <6% of BtNGF was not coupled with QD [supporting information (SI) Fig. 6]. Unless explicitly noted otherwise, we used QDs with a fluorescence emission at 605 nm.

We used PC12 cells to determine whether or not the QD-NGF complex retained the ability to bind specifically to NGF's receptors. PC12 cells, which endogenously express NGF receptors TrkA and P75 (31), were incubated with QD-NGF (0.4 nM) at 37°C for 3 h. Fluorescence imaging of such cells showed many bright puncta,

Author contributions: B.C. and C.W. contributed equally to this work; B.C., C.W., W.C.M., and S.C. designed research; B.C., C.W., L.C., A.R., E.L.B., and W.-P.L. performed research; B.C. contributed new reagents/analytic tools; B.C. analyzed data; and B.C., C.W., and W.C.M. wrote the paper.

The authors declare no conflict of interest.

Abbreviations: NGF, nerve growth factor; TrkA, a receptor tyrosine kinase for nerve growth factor; QD, quantum dot; TIRF, total-internal-reflection fluorescence; DRG, dorsal root ganglia; BtNGF, biotinylated purified NGF; CB/PA, cell body/proximal axon; DA, distal axon.

<sup>h</sup>To whom correspondence may be addressed. E-mail: schu@lbl.gov or ngfv1@stanford.edu.

This article contains supporting information online at [www.pnas.org/cgi/content/full/0706192104/DC1](http://www.pnas.org/cgi/content/full/0706192104/DC1).

© 2007 by The National Academy of Sciences of the USA

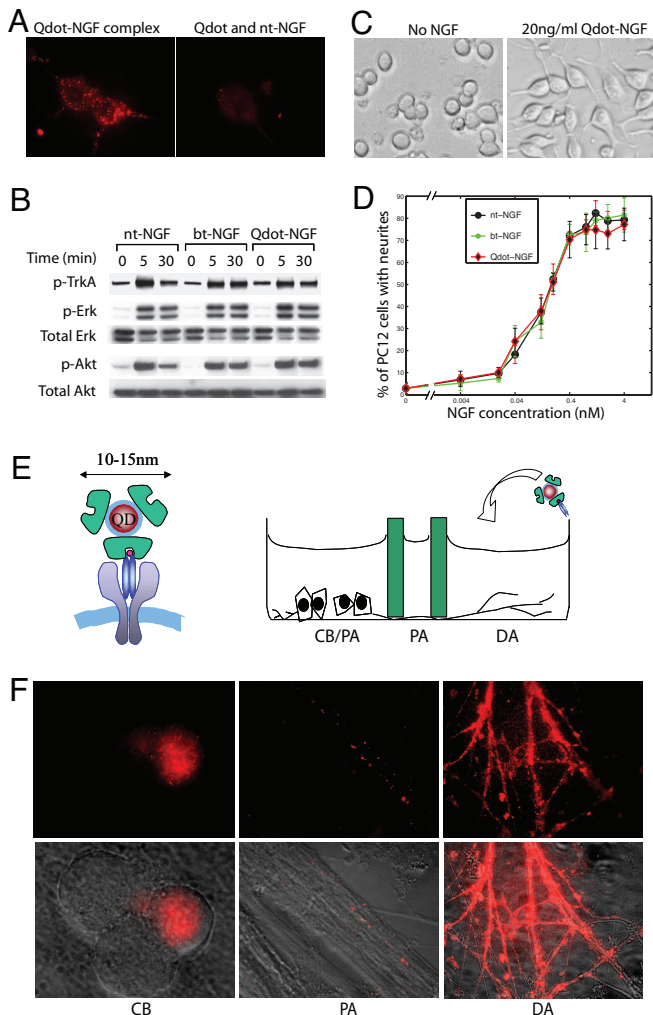


**Fig. 1.** Characterization of QD-NGF biological activity. (A) PC12 cells treated with 0.4 nM of QD-NGF complex for 3 h at 37°C showed bright punctate fluorescence signal even after acid wash (*Left*). PC12 cells treated with the same concentration of QD and native NGF mixture showed fewer if any fluorescent puncta (*Right*). (B) Western blot analysis of phosphorylated TrkA (*p-TrkA*), phosphorylated Erk1/2 (*p-Erk*), and phosphorylated Akt (*p-Akt*) protein levels in PC12 cells in response to the treatment of native NGF, BtNGF, and QD-NGF. The phosphorylation of TrkA peaked at 5 min and decreased slightly at 30 min. Erk1/2 and Akt showed similar level of phosphorylation at 5 min and 30 min. The blots were also probed with antibodies sensitive to total Erk1/2 and total Akt to show equal loading of cell lysate proteins. Application of native NGF, BtNGF and QD-NGF at the same final concentration (2 nM) seemed to activate TrkA, Erk1/2, and Akt to a similar extent. (C) Illustration of QD-NGF bioactivity in PC12-cells. Two days treatment with 0.8 nM QD-NGF stimulated neurite outgrowth in PC12 cells. (D) Quantitative dose-response of PC12 cells to NGF, BtNGF and QD-NGF. The percentage of cells bearing neurites was counted after 2 days of continuous exposure to various concentrations of NGF, BtNGF and QD-NGF. (E) Schematic drawing of a QD-NGF bound to dimerized TrkA receptors (*Left*) and addition of QD-NGF to the DA compartment of the three-chamber DRG neuron culture (CAMP10, *Right*). DA, distal axon; PA, proximal axon; CB, cell body. (F) (*Upper*) Representative live fluorescence images of DRG neuron axons or cell bodies 2 h after the addition of 4 nM QD-NGF to the DA chamber. (*Lower*) Images are the results of these fluorescence images superimposed with their corresponding bright-field images. QD-NGF seems to bind all axons in distal axon chamber. However, only a small portion of the cell bodies and proximal axons are shown to have QD fluorescence, reflecting the fact that not all cell bodies extend their axons into the distal axon compartment.

indicating the presence of QD-NGF (Fig. 1*A Left*). In a companion study, using a mixture of native NGF and QDs (i.e., NGF that was not complexed with QD), we detected very little fluorescence signal

(Fig. 1*A Right*). We also detected robust binding of QD-NGF to COS7 cells that were transfected with TrkA-GFP fusion protein, whereas very little QD-NGF binding was present in COS7 cells that were not transfected (SI Fig. 7). Thus, the presence of NGF was necessary for binding of QD-NGF complexes to NGF receptors.

To determine whether the QD-NGF complex was capable of activating NGF signaling pathways, we compared the responses of PC12 cells to NGF, BtNGF and QD-NGF. Similar to the effect of adding NGF or BtNGF alone, QD-NGF showed robust activation of TrkA, as well as Erk1/2 and Akt, two downstream signaling proteins that play critical roles in NGF signaling pathways (Fig. 1*B*). Consistent with a recent report (32), QD-NGF was able to stimulate neurite outgrowth in PC12 cells (Fig. 1*C*). Judged by the dose-response results for neurite outgrowth, the activity of QD-NGF was comparable with that of BtNGF as well as native NGF (Fig. 1*D*). On the basis of these data, we conclude that QD-NGF is biologically active and induces physiologically significant responses.

**QD-NGF Is Internalized at the Axon Terminal and Retrogradely Transported to the Cell Body.** To show that the QD-NGF complex can be internalized at axon terminals and retrogradely transported to neuron cell bodies, we used CAMP10 Campanot chambers (33) to culture embryonic dorsal root ganglion (DRG) neurons (Fig. 1*E*). The three separate compartments, depicted in Fig. 1*E*, contain (*i*) cell bodies and their most proximal axons (CB/PA); (*ii*) proximal axons alone (PA); (*iii*) distal axons (DA) alone. QD-NGF (4 nM) was applied exclusively to the DA compartment. For QD-NGF to gain access to cell bodies, it must be internalized in distal axons and retrogradely transported within axons. A five hour incubation period was chosen to ensure that a sufficient number of QD-NGF complexes were transported to the CB/PA chamber. At the conclusion of the incubation, all compartments were washed and cells were fixed for fluorescence imaging. Fig. 1*F* shows that QD-NGF was bound to most if not all axons in the DA compartment, as evidenced by a prominent QD fluorescence signal over individual axons and clusters of axons. In the CB/PA compartment, QD-NGF was observed only in some proximal axons and cell bodies. We estimated that ≈25% of cell bodies and ≈10% of proximal axons were labeled. This labeling efficiency probably reflected the fact that not all cell bodies extended axons into the distal chamber and is further evidence that there was no leakage between CB/PA and DA compartments.

As a control, we applied a mixture of native NGF and QDs, the same final concentrations as above, to distal axons. We found <5% of the QD signals in the CB/PA compartment as compared with QD-NGF complexes. In addition, we noted that retrograde transport of QD-NGF was almost completely eliminated (≈1% of normal transport) when axons in the DA compartment were pretreated with 200 nM K252a, a known inhibitor of Trk tyrosine kinase. This finding is consistent with previous studies (10, 34) that Trk activation is required for NGF internalization. Given their biological activity and marked stability, the QD-NGF complex provides a useful tool for examining the axonal transport of NGF.

**QD-NGF Containing Endosomes Exhibit Stop-and-Go Motion.** For imaging in live neurons, we combined a pseudoTIRF microscope with a temperature-controlled stage constructed to hold the compartmented culture in the CAMP10 chamber. PseudoTIRF (see *Materials and Methods*) is characterized by a low fluorescence background, but allows for visualization of structures located up to a few micrometers from a glass-water interface; beyond the illumination range of conventional TIRF microscopy. Our measurements were performed at 34°C. QD-NGF (final concentration 1 nM) was applied exclusively to the DA compartment. It took ≈40 min for the first few QD-NGF-containing endosomes to reach the CB compartment, which is comparable with the 30- to 60-min interval needed for transport of <sup>125</sup>I-labeled NGF (16). We confined fluorescence imaging of QDs exclusively to the CB/PA

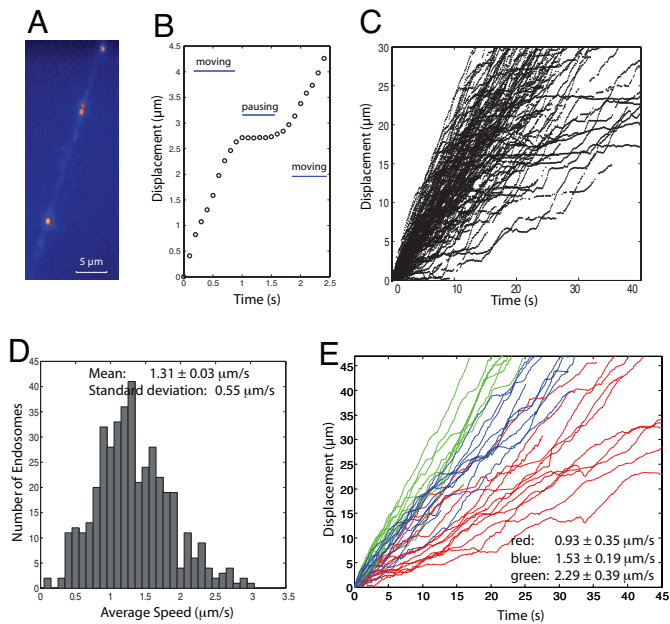


**Fig. 2.** Live imaging reveals that endosomes containing QD-NGF exhibit stop-and-go motion (see real-time SI Movies 1–5). (A) A typical axon showing four moving endosomes that contained QD-NGF in pseudocolor. The background fluorescence outlines the axon in this picture. (B) Trajectory of a typical endosome, showing a switch between moving and pausing. (C) Trajectories of 120 endosomes showing that the moving speed and the duration of pauses vary greatly from one endosome to another. (D) The average speed of endosomes containing QD-NGF varied from 0.2 to 3  $\mu\text{m/s}$ . (E) Comparison of endosomes moving in three different axons. The trajectories of endosomes within the same axon are denoted with the same color (red, blue or green). The variability between different axons is significantly larger than the spread of velocities in the same group.

chamber to ensure that all of the QD-NGF complexes observed were internalized and transported from the DA chamber.

Live-imaging revealed that endosomes containing QD-NGF moved in a stop-and-go manner (see live imaging SI Movies 1–5). A typical axon, containing four QD-NGF endosomes is shown in Fig. 2A. The time-lapse trajectory shown in Fig. 2B, featuring frequent switching from moving to pausing and then to moving, was typical. In the vast majority of cases ( $\approx 90\%$ ), QD-NGF endosomes moved exclusively toward the cell body. Even when anterograde movement was observed, it generally persisted for a very short time ( $\approx 0.5$  s) and resulted in only small displacements.

The moving speed and the duration of pauses varied greatly from one endosome to another (Fig. 2C). At a QD-NGF concentration of 1 nM, the average speed, which included both periods of active movement and pausing, measured  $1.31 \pm 0.03 \mu\text{m/s}$  (mean and uncertainty of the mean). Pausing accounted for  $\approx 30\%$  of time; the speed during active movement was  $2.11 \pm 0.05 \mu\text{m/s}$ . Among different endosomes, the average speeds varied from  $0.2 \mu\text{m/s}$  to  $3 \mu\text{m/s}$  and the moving speeds varied from  $0.5 \mu\text{m/s}$  to  $5 \mu\text{m/s}$ . Fig. 2D shows the distribution of average speeds. The variation in the speeds could result from differences in the resistance to movement within axons, in the motors used, or in the number of motors engaged.

**Endosomes in an Axon Move at a Similar Speed.** Fig. 2E shows the movement of 39 QD-NGF containing endosomes in three different axons. Endosomes moving in the same axon are plotted in the same color. All endosomes showed typical stop-and-go motion. The green traces showed that endosomes in this axon moved with an average speed of  $2.29 \pm 0.39 \mu\text{m/s}$ . The endosomes shown in the red traces paused longer and more frequently, resulting in an average

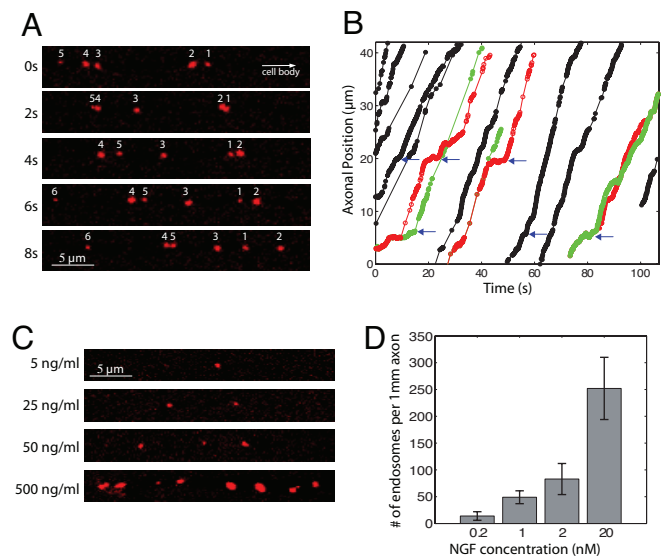


**Fig. 3.** Transport dynamics and concentration dependence of QD-NGF containing endosomes. (A) Time-lapse video images (after background subtraction) of endosomes traveling on the same axon. Five endosomes were visible at the beginning of the video recording, and the sixth endosome came into the field of view after 6 s. The endosomes are numbered according to their axonal positions at the start of the video recording. After 4 s, two fast moving endosomes (no. 2 and no. 5) passed the slower ones (no. 1 and no. 4). The white arrow indicates that direction of motion was toward the cell body. (B) Trajectories of fifteen endosomes moving in the same axon through the same field of view. The majority of endosomes move independently (black circles). Endosomes moving together or passing another endosomes are shown in red and green for clarity. The blue arrows indicate the places where some trajectories paused at the same axonal location. (C) The number of endosomes in a fixed length of axon increases with QD-NGF concentration. Typical images showing the density of endosomes increases with QD-NGF concentration (see real-time SI Movies 1–5). At 20 nM concentration, the fluorescence intensity of individual endosomes contained QD-NGF increased significantly. (D) Average number of endosomes per 1 mm of axons increases with increased QD-NGF concentration ranging from 0.2 to 20 nM.

speed of  $0.93 \pm 0.35 \mu\text{m/s}$ , less than half of that for the axon whose traces are shown in green. Thus, the average speed of endosomal movement seems to vary considerably between axons, suggesting differences in the ability of individual axons to support endosomal traffic.

**Some Endosomes in the Same Axon Pause at the Same Apparent Axonal Location.** In many axons, several QD-NGF-containing endosomes were present and moving. They often exhibited a pattern of movement that resembled multilane highway traffic. Most endosomes moved independently of one another: fast moving ones passed those moving more slowly or that were paused. Fig. 3A shows a number of endosomes moving in the same axon. Each of the two rapidly moving endosomes (no. 2 and no. 5) was observed to pass the ones initially in front of them. We also noted examples in which paused endosomes seemed to obstruct the advance of other endosomes. Occasionally, two or more endosomes located very near one another traveled at the same speed for a few seconds before eventually separating. Fig. 3B plots the displacements vs. time for 15 endosomes moving in a portion of one axon during a period of 2 min. Red and green lines denote instances in which endosomes passed each other. Interestingly, some, but not all, endosomes that traveled in the same axon seemed to pause at the same apparent location (as shown by the blue arrows in Fig. 3B). This unexpected finding raises the possibility that pausing may be influenced by local structural features in axons.

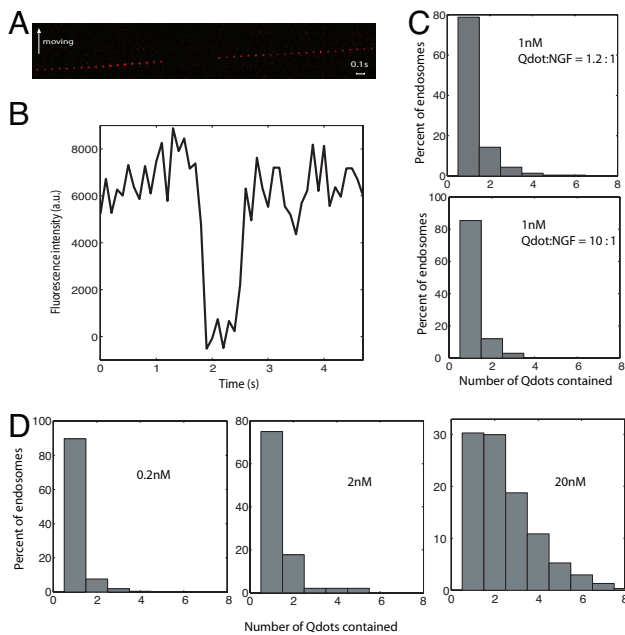


**Fig. 4.** Quantification of the number of QD-NGFs contained in individual endosomes. (A) “Photo-blinking” of a single QD particle. A time sequenced (every 0.1 s) images of a QD-NGF containing moving endosome. The sudden disappearance of QD fluorescence for 0.7 s in the middle is due to the intrinsic photo-blinking property of QDs. Time trace of the fluorescence intensity of the endosome is shown in B. The fluorescence intensity of the endosome is consistent with the intensity of a single QD particle. The sudden decrease of the fluorescence signal to background levels (“blinking”) is the signature of a single QD particle. (C) Distribution of the number of QD particles contained in endosomes when QD was mixed with BtNGF at molar ratios of 1.2:1 and 10:1. The number of QD particles in each endosome was quantified by measuring both the blinking events and the fluorescence intensity. (D) Distribution of the number of QD particles in endosome at the QD-NGF concentration of 0.2, 2 and 20 nM. The majority of endosomes contained a single QD-NGF at 0.2 and 2 nM. At 20 nM, ≈30% of endosomes contained just one QD-NGF and the rest contained two or more QD-NGF conjugates.

**The Number of QD-NGF-Containing Endosomes Increases with QD-NGF Concentration.** The number of QD-NGF-containing endosomes observed in a fixed length of axon increased significantly with increasing QD-NGF concentration in the range of 0.2 to 20 nM (Fig. 3C). We detected no significant change in the stop-and-go pattern of movement, or the average speed of movement, of endosomes at different QD-NGF concentrations. QD-NGF containing endosomes were readily detected at 0.2 nM, a concentration that induced a robust neurite outgrowth response in PC12 cells (Fig. 1D). The distance between adjacent QD-NGF endosomes under this condition averaged ≈69 μm. With increasing QD-NGF concentration, the number of endosomes traveling in the axon increased (Fig. 3C and D). The number of endosomes per 1 mm of axon was estimated to be ≈14 at QD-NGF concentration of 0.2 nM, ≈49 at 1 nM, and ≈83 at 2 nM and ≈252 at 20 nM. These observations indicate that axonal transport of NGF is not saturated even at concentrations that are beyond what is considered the physiological range.

**The Majority of Endosomes Contain a Single QD-NGF.** The photo-blinking property of QD fluorescence (35) (i.e., on-off-on fluorescence emission) allowed us to determine the number of QD-NGF molecules per endosome. Under our experimental conditions, the QD spends ≈5–10% of time in a dark state that does not emit fluorescent light. Fig. 4A shows time-lapse images of an endosome containing QD-NGF; the fluorescence intensity for this QD was plotted in Fig. 4B. The sudden and complete loss of fluorescence in

the middle 7 frames denotes the blinking of a single QD (Fig. 4A and B). Endosomes containing a single QD were identified individually by checking for blinking events for more than five consecutive frames (0.5 s). For endosomes that did not blink, the number of QD-NGF complexes contained could be determined by comparing the fluorescence intensity to that for endosomes containing a single QD-NGF that did blink. Because of the variation in the fluorescence intensity of a single QD, this number must be regarded as an approximation. Using these measures, the majority (≈80%) of endosomes in cultures treated with NGF at 1 nM, a concentration at which the neurite outgrowth response was maximal, contained a single QD (Fig. 4C Top), of which 90% exhibited characteristic photo-blinking. It should be noted that axons were not always parallel to the glass surface so that QD-containing endosomes were seen to come in and out of the plane of focus as they traveled along the axon; this out-of-focus movement caused fluorescence intensity to fluctuate and sometimes lead to the complete disappearance of QD fluorescence. However, these events were easily distinguished from blinking by the much slower variation of fluorescence intensity.

To confirm that most endosomes contained a single QD-NGF complex, we mixed QD605-NGF (emission 605 nm) with QD705-NGF (emission 705 nm) at a 1:1 ratio and applied the mixture to the DA chamber of the compartmented culture. If most endosomes contain two or more QD-NGF complexes, we would expect to see a large fraction of them containing both QD605 and QD705. A 650-nm dichroic mirror spectrally resolved fluorescence emission from QD605 or QD705. The fluorescence emission was further filtered by passing through appropriate QD emission filters. Endosomes containing QD605 and those containing QD705 were observed in the CB/PA compartment. Whereas a few of endosomes were observed that contained both QD605 and QD705, the vast majority (≈90%) contained either QD605 or QD705 (data not shown). This result further strengthens the conclusion that majority of endosomes contained a single QD-NGF.

To further confirm that a single QD-NGF complex transported in an axon needs only a single NGF dimer (each QD contains several streptavidin binding sites, as indicated in Fig. 1E.), we prepared a QD-NGF mixture using a 10:1 molar ratio of QD to BtNGF. Under this coupling condition, <5% of QD-NGF complexes would be expected to contain more than one NGF dimer. Endosomes containing a single QD-NGF complex were readily detected. Statistical analysis revealed that 85% of endosomes contained a single QD at this stoichiometry of QD to NGF (Fig. 4C Bottom). Our finding strongly suggests that a single NGF dimer resides within most retrogradely transported endosomes. In light of earlier studies pointing to the ability to regenerate NGF signaling during endosomal transport (10), it is possible that a single NGF dimer can sustain signaling from endosomes during transport.

We investigated further how concentration influenced the number of QD-NGF complexes contained within endosomes. Fig. 4D displays the distribution of the number of QD-NGF complexes present in individual endosomes at each of several concentrations. At concentrations of 0.2 and 1.0 nM, the majority of endosomes contained a single QD-NGF complex (Fig. 4D Left and Center). At 20 nM, individual puncta showed notably enhanced fluorescence intensity (Fig. 3C). Whereas it was difficult to define precisely the number of QD-NGF complexes/endosome at 20 nM, we estimate that ≈30% still contained just one (Fig. 4D Right).

**Most QD-NGF Is Transported in Axons in Small 50- to 150-nm Vesicles.** One set of hypotheses for retrograde axonal transport of NGF states that NGF and its signaling proteins are transported in complex vesicles such as multivesicular bodies, lysosomes, or macropinosomes (8, 20, 36). To examine the endocytic compartment(s) that immediate the retrograde transport of QD-NGF, we took advantage of the fact that QD has an electron dense core that can be visualized under electron microscopy (EM) (37). DRG neurons

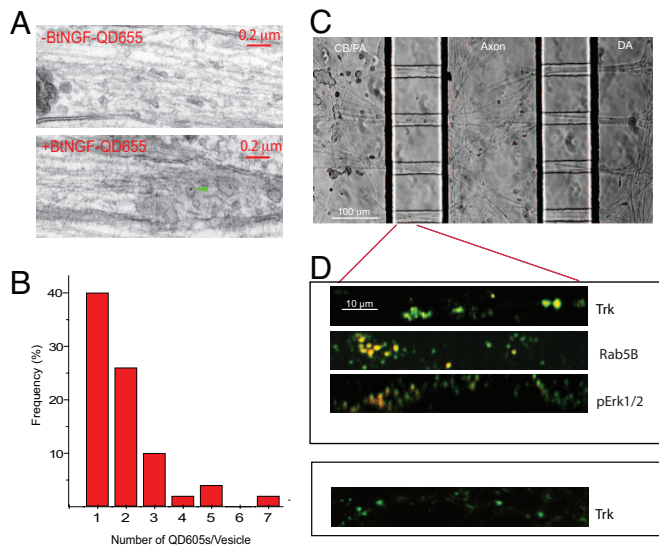


**Fig. 5.** EM and immunostaining analysis of endosomes containing QD-NGF. DRG neurons treated with QD-NGF were fixed, embedded and processed for ultrathin sectioning. (A) A representative EM image of a cross-section of the proximal axon portion showing that it contained many small vesicles (50–150 nm in diameter). One vesicle contained QD (arrows). (B) Out of 84 QD containing vesicles, most had 1–2 QD particles. (C) A representative image of DRG neurons cultured inside a microfluidic device. Axons were able to extend across two columns of microgrooves into the distal axon chamber. (D) After QD-NGF was added to the DA chamber for 2 h, all chambers were rinsed and fixed for immunostaining by using the indicated primary antibodies. A secondary antibody-Alexa 488 conjugate (green) was used to reveal these primary antibodies (green). We confined our observations to the sections of axons leading to the cell body in the microgrooves. The colocalization (yellow) between QD-NGF (red) and Trk, Rab5B and pErk1/2 (all green) is extensive (three panels in *Upper*). When QD was omitted, we were unable to detect a red signal but the green signals for the other markers such as Trk (*Lower*) remained.

were cultured in the microfluidic chamber and treated with 2 nM QD-NGF, as described above. Samples were rinsed and fixed for EM analysis by using established protocols (37). A grid with pure QD-NGF was also imaged and used as a size guidance to determine whether the black dots inside the vesicles were QDs. As shown in Fig. 5A, a typical DRG axon has a diameter of  $\approx 1 \mu\text{m}$ . QDs were often seen as  $\approx 5 \text{ nm}$  dark dots (arrow in Fig. 5A). QDs were most easily seen in vesicles of 50–150 nm in diameter (mean =  $59 \pm 35 \text{ nm}$ ;  $n = 84$ ), that were uncoated and whose lumen was clear. As a control, these distinctive electron-dense dots were absent in samples that were treated with NGF only. In agreement with the results of live imaging studies (Fig. 4D), cells treated with 2 nM QD-NGF showed that most QD-NGF containing vesicles contained 1 or 2 QDs (Fig. 5B). This result was independently verified at the Marine Biological Laboratory (SI Fig. 8). We conclude that under the condition of our experiments, small vesicles (50–150 nm) are responsible for most retrograde axonal transport of QD-NGF in DRG axons.

**QD-NGF Colocalizes with Trk, pErk1/2, and Rab5B in Proximal Axons.** To show that QD-NGF containing endosomes carry the NGF signal, we examined the distribution of these endosomes with respect to that of signaling proteins that were shown to mediate NGF signaling and associate with retrogradely transported endosomes under physiological conditions (11, 38). For this study, we adopted a modified version of microfluidic nerve cell chamber (39), which enhances the ability to image and track QD signals (Fig. 5C).

Microfluidic DRG cultures were deprived of NGF and serum for 24 h before QD-NGF was added to the distal axon compartment.

After 2 h of incubation, cells were extensively rinsed, fixed and stained with antibodies to Trk, pErk1/2 (i.e., activated Erk1/2) by using established protocols (11). Rab5, a marker of early endosomes, was also examined. The primary antibodies were detected with Alexa 488-secondary antibody conjugates (green). Axons in microgrooves were examined by using confocal microscopy. As shown in Fig. 5D, QD-NGF (red) was essentially completely colocalized with both Trk (top image in *Upper*) and Rab5B (middle image in *Upper*). However, not all Trk, Rab5B signals were marked by QD-NGF. This observation may be explained, at least in part, by the visualization of Trk and Rab5 not undergoing retrograde transport. Among the 845 puncta positive for Rab5B, 172 ( $\approx 20\%$ ) were also positive for QD-NGF; among the 378 puncta positive for Trk, 230 ( $\approx 61\%$ ) were also marked by QD-NGF. Like Trk and Rab5, QD-NGF was colocalized with pErk1/2. Of the puncta positive for pErk1/2,  $\approx 77\%$  (445/582) were also positive for QD-NGF. Of note, some complexes were present in endosomes that failed to stain positively for antibodies, or did so only weakly. These results are evidence that QD-NGF is transported in early endosomes that also carry Trk and activated Erk1/2.

## Discussion

The use of technologies such as (*i*) quantum dots labeled NGF, (*ii*) microfluidic chambers for neuronal culture, (*iii*) pseudoTIRF microscopy, and (*iv*) single molecule detection and analysis, provided us with the opportunity to study NGF retrograde transport in great details. The “blinking” property and electron-dense core of QDs led to the surprising discovery that most endosomes carried a single NGF dimer at physiological concentrations. In view of recent findings revealing impaired NGF transport in mouse models of giant axonal neuropathy (40, 41) and Down syndrome (42), these technologies may well facilitate studies of those systems in which failed NGF transport contributes to neurodegeneration.

We are aware of the potential that QD labeling could alter trafficking and signaling of NGF and have carefully considered this issue in carrying out these studies and in interpreting our findings. To this end, we have shown that QD-NGF binds specifically to NGF receptors and activates NGF signaling pathways in a fashion similar to unmodified NGF in PC12 cells. We have also demonstrated that QD-NGF can be internalized at axon terminals and retrogradely transported to neuron cell bodies. Also, the average moving speed of QD-NGF within the axon ( $\approx 1.3 \mu\text{m}/\text{s}$ ) is in line with speeds reported in the literature using  $^{125}\text{I}$ -NGF. We further used immunofluorescence method to show that QD-NGF colocalized with Rab5, TrkA, and pErk1/2. Taken together, these findings suggest that QD labeling unlikely altered the signaling or trafficking of NGF. Although conventional labeling methods have been used with good effect to trace NGF transport, one can readily envision that QDs will now be used routinely.

## Materials and Methods

**Production of Biotinylated NGF.** Native NGF was purified from mouse submaxillary glands following a published protocol (28). NGF was biotinylated via carboxyl group substitution by using EZ-link biotin-PEO-amine and the coupling reagent 1-ethyl-3-(3-dimethylaminopropyl)-carbodiimide (EDAC) (Pierce Biotech, Rockford, IL) as described by Bronfman *et al.* (29). The reaction routinely yielded an average of three biotin molecules per NGF dimer as assayed using FluoroReporter Biotin Quantification kit (Molecular Probes, Portland, OR). Streptavidin-quantum dots (QD605, QD705), secondary antibodies conjugated to Alexa 488 were purchased from Invitrogen (Carlsbad, CA). Mouse IgGs against McTrk, pErk1/2, rabbit IgGs against Rab5B were purchased from Santa Cruz Biotechnology (Santa Cruz, CA). Rabbit IgGs against phosphorylated Trk, phosphorylated Akt and total Akt were from Cell Signaling Technology (Danvers, MA).

**PC12 Cell Culture and Rat E16 DRG Culture.** PC12 cells and were maintained as described (38). Embryonic DRG neurons were isolated from Sprague–Dawley fetal rats [embryonic day (E) 15 and 16], and cultured in DMEM containing 10% FCS and 50 ng/ml NGF as described by Chan *et al.* (43). For compartmented culture, a three-chamber Teflon divider (CAMP10, Tyler Research, Edmonton, Alberta, Canada) was sealed to a collagen-coated coverslip with silicone grease. Dissociated DRG neurons were plated into the left most chamber. Axons crossed under the first grease barrier into the central chamber within 5–7 days and reached the right chamber (distal axon chamber) after crossing the second grease barrier in ≈2 weeks. We also used modified microfluidic nerve cell chambers for imaging and EM analysis (39). Unless indicated otherwise, 3- to 4-week-old cultures of DRG neurons were used in all experiments.

**Immunofluorescence Staining and EM Analysis.** After addition of QD-NGF to the axons in the distal chamber, cultured DRG neurons were fixed in 4% paraformaldehyde, permeabilized in 0.2% Triton X-100 in PBS, and blocked with 5% normal goat serum for 1 h before the application of rabbit or mouse antibodies against various proteins. The primary antibody was visualized by using an appropriate secondary antibody-Alexa 488 conjugate. For EM analysis, a published protocol was followed [Gièpmans *et al.* (37)]. Electron micrographs were taken from 80-nm-thick sections at 120 kV with a transmission electron microscope (Model: JEM-1200 EX II; Jeol Ltd.) at the EM facility of Stanford University, and with a JEOL CX200 at the Marine Biological Laboratory, Woods Hole, MA.

**PseudoTIRF Microscope and Live Imaging.** An inverted microscope (Nikon TE2000U) was modified for pseudoTIRF illumination. The

laser beam (532 nm) was first expanded to 3 cm and then focused at the back focal plane of the objective lens (Planapo ×60, 1.45 NA, Olympus). The incident angle was adjusted to be slightly smaller than the critical angle so that the laser beam could penetrate ≈1 μm into the aqueous solution.

To image transport of QD-NGF in live neurons, the compartmented culture was supplied with QD-NGF in the DA chamber for 3 h. The compartmented culture was mounted on a fabricated microscope stage without removing the Teflon divider. Fluorescence images were filtered with a QD605/20 emission filter. Time-lapse images were acquired by using an EMCCD camera (Cascade 512B; Roper Scientific) at the speed of 10 frames per second. For dual imaging of QD605-NGF and QD705-NGF, the fluorescence emission was split by a 650 nm dichroic mirror. The two spectrally resolved copies of the microscope image were further filtered by passing through QD605/20 or QD705/20 emission filters and relayed onto halves of the EMCCD camera. For further details, see *SI Materials and Methods*.

B.C. thanks Drs. Harold Kim, Janice S. Valletta, Keith Weninger, and Wei-Hau Chang for their generous assistance for her research. E.L.B. thanks Jean Edens at Caltech for her skill with thin-sectioning for electron microscopy. This work was supported by National Science Grants PHY-0420752 and PHY-0647161, National Aeronautics and Space Administration Grant NNC04GB49G, National Institutes of Health (NIH) Grants NS24054, NS38869, AG16999, NS046810, NS05537, and GM47368, The Larry L. Hillblom Foundation, The Deane Johnson Fund, The Adler Foundation, Dart Neurosciences LLP, and The Moore Foundation. B.C. acknowledges support from the Pathway to Independence Career Award from NIH.

1. Sofroniew MV, Howe CL, Mobley WC (2001) *Annu Rev Neurosci* 24:1217–1281.
2. Miller FD, Kaplan DR (2002) *Science* 295:1471–1473.
3. Ginty DD, Segal RA (2002) *Curr Opin Neurobiol* 12:268–274.
4. Beattie EC, Zhou J, Grimes ML, Bunnett NW, Howe CL, Mobley WC (1996) *Cold Spring Harbor Symp Quant Biol* 61:389–406.
5. Grimes ML, Beattie E, Mobley WC (1997) *Proc Natl Acad Sci USA* 94:9909–9914.
6. Zweifel LS, Kuruvilla R, Ginty DD (2005) *Nat Rev Neurosci* 6:615–625.
7. Kuruvilla R, Zweifel LS, Glebova NO, Lonze BE, Valdez G, Ye H, Ginty DD (2004) *Cell* 118:243–255.
8. Claude P, Hawrot E, Dunis DA, Campenot RB (1982) *J Neurosci* 2:431–442.
9. Watson FL, Heerssen HM, Moheban DB, Lin MZ, Sauvageot CM, Bhattacharyya A, Pomeroy SL, Segal RA (1999) *J Neurosci* 19:7889–7900.
10. Ye H, Kuruvilla R, Zweifel LS, Ginty DD (2003) *Neuron* 39:57–68.
11. Delcroix JD, Valletta JS, Wu C, Hunt SJ, Kowal AS, Mobley WC (2003) *Neuron* 39:69–84.
12. Ure DR, Campenot RB (1997) *J Neurosci* 17:1282–1290.
13. Reynolds AJ, Bartlett SE, Hendry IA (1998) *Brain Res* 798:67–74.
14. Howe CL, Mobley WC (2004) *J Neurobiol* 58:207–216.
15. MacInnis BL, Campenot RB (2002) *Science* 295:1536–1539.
16. Senger DL, Campenot RB (1997) *J Cell Biol* 138:411–421.
17. von Bartheld CS (2001) *Methods Mol Biol* 169:195–216.
18. Korschning S, Thoenen H (1983) *Neurosci Lett* 39:1–4.
19. Reynolds AJ, Hendry IA (1999) *Brain Res Brain Res Protoc* 3:308–312.
20. Weible MW, 2nd, Bartlett SE, Reynolds AJ, Hendry IA (2001) *Cytometry* 43:182–188.
21. Lalli G, Schiavo G (2002) *J Cell Biol* 156:233–239.
22. Tani T, Miyamoto Y, Fujimori KE, Taguchi T, Yanagida T, Sako Y, Harada Y (2005) *J Neurosci* 25:2181–2191.
23. Shao Y, Akmentin W, Toledo-Aral JJ, Rosenbaum J, Valdez G, Cabot JB, Hilbush BS, Halegoua S (2002) *J Cell Biol* 157:679–691.
24. Pinaud F, Michalet X, Bentolila LA, Tsay JM, Doose S, Li JJ, Iyer G, Weiss S (2006) *Biomaterials* 27:1679–1687.
25. Lidke DS, Nagy P, Heintzmann R, Arndt-Jovin DJ, Post JN, Grecco HE, Jares-Erijman EA, Jovin TM (2004) *Nat Biotechnol* 22:198–203.
26. Bonneau S, Dahan M, Cohen LD (2005) *IEEE Trans Image Process* 14:1384–1395.
27. Fu A, Gu W, Larabell C, Alivisatos AP (2005) *Curr Opin Neurobiol* 15:568–575.
28. Mobley WC, Rutkowski JL, Tennekoon GI, Gemski J, Buchanan K, Johnston MV (1986) *Brain Res* 387:53–62.
29. Bronfman FC, Tcherpakov M, Jovin TM, Fainzilber M (2003) *J Neurosci* 23:3209–3220.
30. Rosenberg MB, Hawrot E, Breakefield XO (1986) *J Neurochem* 46:641–648.
31. Zhuang X, Bartley LE, Babcock HP, Russell R, Ha T, Herschlag D, Chu S (2000) *Science* 288:2048–2051.
32. Vu TQ, Maddipati R, Blute TA, Nehilla BJ, Nusblat L, Desai TA (2005) *Nano Lett* 5:603–607.
33. Campenot RB (1977) *Proc Natl Acad Sci USA* 74:4516–4519.
34. Bhattacharyya A, Watson FL, Bradlee TA, Pomeroy SL, Stiles CD, Segal RA (1997) *J Neurosci* 17:7007–7016.
35. Hohng S, Ha T (2004) *J Am Chem Soc* 126:1324–1325.
36. Valdez G, Akmentin W, Philippidou P, Kuruvilla R, Ginty DD, Halegoua S (2005) *J Neurosci* 25:5236–5247.
37. Gièpmans BN, Deerinck TJ, Smarr BL, Jones YZ, Ellisman MH (2005) *Nat Methods* 2:743–749.
38. Wu C, Lai CF, Mobley WC (2001) *J Neurosci* 21:5406–5416.
39. Taylor AM, Blurton-Jones M, Rhee SW, Cribbs DH, Cotman CW, Jeon NL (2005) *Nat Methods* 2:599–605.
40. Bomont P, Koenig M (2003) *Hum Mol Genet* 12:813–822.
41. Ding J, Allen E, Wang W, Valle A, Wu C, Nardine T, Cui B, Yi J, Taylor A, Jeon NL, *et al.* (2006) *Hum Mol Genet* 15:1451–1463.
42. Salehi A, Delcroix JD, Belichenko PV, Zhan K, Wu C, Valletta JS, Takimoto-Kimura R, Kleschevnikov AM, Sambamurti K, Chung PP, *et al.* (2006) *Neuron* 51:29–42.
43. Chan JR, Rodriguez-Waitkus PM, Ng BK, Liang P, Glaser M (2000) *Mol Biol Cell* 11:2283–2295.

